Korean J. Chem. Eng., 36(12), 2060-2073 (2019)
DOI: 10.1007/s11814-019-0393-9

pISSN: 0256-1115
eISSN: 1975-7220

Competency of chlorination roasting coupled water leaching process for potash recovery from K-feldspar: Mechanism and kinetics aspects

Sandeep Kumar Jena*,,†, Nilima Dash*, Akshaya Kumar Samal***, and Pramila Kumari Misra**,†**

*CSIR-Institute of Minerals and Materials Technology, Bhubaneswar-751013, India
**School of Chemistry, Sambalpur University, Jyoti Vihar-768019, India
***Centre for Nano and Materials Sciences, Jain University, Bangalore-562 112, India
(*Received 4 June 2019 • accepted 22 September 2019*)

Abstract−Potassium is an important mineral for biological functions. In this study, potassium was recovered from a low-grade potash mineral, feldspar through chlorination roasting followed by water leaching. NaCl and $CaCl_2$ were used as additives for chlorination roasting independently. The characterizations throughout the studies were carried out using a series of analytical and spectral techniques like XRD, SEM, FTIR, and Raman spectroscopy. The effects of various experimental parameters such as particle size, roasting temperature, amounts of additives, and water leaching on potassium extraction were evaluated. Water leaching was found to be independent of leaching time, temperature, and agitator speed. During roasting, the formation of water-soluble phase was evident; this phase subsequently disappeared on water leaching. The potassium extraction kinetics in the presence of both the additives was satisfactorily corroborated by Ginstling-Brounshtein model. The activation energies for $CaCl_2$ and NaCl roasting were calculated to be 90 and 122 kJ/mole, respectively. Under the same experimental conditions, 86% of potassium extraction (as potash value) was accomplished using $CaCl_2$ as the additive, whereas the extraction in presence of NaCl was only up to 44%. The mechanism of potassium extraction was elucidated; the superior effectiveness of $CaCl_2$ over NaCl in the extraction process was also explained.

Keywords: Chlorination Roasting, Feldspar, Extraction Kinetics, Potassium, Roast-leach Method, Ginstling-Brounshtein Model

INTRODUCTION

An abrupt increase in population growth around the globe demands a proportionate increase in food production. But the quality of soil is steadily deteriorating due to natural and man-made activities; particularly, the micronutrient content of soil is decreasing conspicuously. This disparity in increased demand for food production and decreased quality of soil lead to an adverse effect on agriculture. To increase food production the deficiency of the micronutrients is very often overcome by supplementing with commercially available micronutrients [1]. Similar to other micronutrients such as nitrogen and phosphorus, potassium plays an important role in the growth of plants and crops. Potassium contributes to the yield, color, taste, and disease-resistant power of food crops significantly. Therefore, the requirement for potassium in fertilizers is increasing steadily. A literature survey shows that the global demand for potassium in the agriculture sector would grow at a rate of 2.5-3% annually [2,3]. Extensive studies have been conducted on improved food production using many potassium fertilizers [4-6]. The fertilizer industry is paying much attention to the resources and benefits of potassium. Because of the unavailability of indigenous potassium sources, India imports most of its potassium requirement from other countries. As a result, India is a major buyer of potassic fertilizers in the global market [7]. Since it is an agriculture-based country, India's economy is mostly dependent on agriculture. Therefore, the production of potassium from indigenous sources has become indispensable in India.

Diverse resources of potassium such as sea water, certain clays, and rock-forming minerals and high-tech potassium extraction technologies have been extensively reviewed in the literature [8-10]. Few extraction processes for potassium from sea water have been reported [11-14], but they are not profitable due to the low content of potassium in sea water (392 ppm of K at 3.5% salinity). Some naturally occurring minerals such as feldspar, nepheline syenite, mica, glauconitic sandstone, granites, orthoclase, and kainite have significant amounts of potassium; different methods for the extraction of potassium from these minerals such as flotation [15-18], chemical leaching [19,20], roasting followed by leaching [21,22,31] and bioleaching [23,24] are reported to be cost-effective.

The most common mineral (around 50% of earth's crust) is feldspar, and its major constituents are O, Al, Si, K, Na, and Ca with the potassium content in the range 5-15%. Since feldspar occurs abundantly in India, the potassium extraction from it has high potential. Feldspar is mostly used as a flux in the glass and ceramics industries after removing the major impurities such as iron [25]. The three end-members of feldspar family are K-feldspar ($KAlSi_3O_8$), albite ($NaAlSi_3O_8$), and anorthite ($CaAl_2Si_2O_8$). The structure of feldspar is influenced by the ionic radius, ordering of Al-Si tetrahedra, and presence of charge balancing ions such as K^+, Na^+, Ca^{+2}, or Ba^{+2}. But due to the uniform distribution of K^+ throughout the crystal structure of feldspar as a charge balancing cation, the extraction of

†To whom correspondence should be addressed.
E-mail: sandeepjena@immt.res.in, sandeepimmt@gmail.com, pramilakmisra@gmail.com, pramilamisra@rediffmail.com
Copyright by The Korean Institute of Chemical Engineers.

Table 1. Extraction of potassium values from feldspar and other potash bearing minerals by the roast-leach method

Mineral	Reagents/Additives	Expt. conditions	K_2O %, Extraction	References
Feldspar	$CaCl_2$ and NaCl	800 °C, 1 hr roasting, water leaching	95.35%	[30]
Feldspar	$CaCl_2$	800°C, 1 hr roasting, hot water leaching	84.7%	[32]
Feldspar	Na_2CO_3 or ($CaCO_3$+$CaSO_4$)	Roasting-leaching	80%	[34]
Feldspar/K-bearing minerals	$CaCO_3$/NaCl/$CaCl_2$	825-950 °C roasting, water leaching	60-80%	[35]
Feldspar	Na_2CO_3	875 °C, 40 min roasting, water leaching	98%	[36]
Glauconitic sandstone	$CaCl_2$	750-800 °C roasting, water leaching	90%	[27]
Nepheline syenite	$CaCl_2$	900 °C, 30 min roasting, water leaching	99.6%	[21]

potassium value from this mineral is difficult unless the crystal structure is distorted. Among all the possible extraction methods for potassium, the roast-leach method is a convenient method to release the unlocked potassium values from the complex matrix of feldspar [26-28]. The roast-leach method includes the mixing of fine feldspar powder with required amounts of additives such as $NaNO_3$, $MgSO_4$, $CaCO_3$, $CaCl_2$, NaCl, or Na_2CO_3 followed by high-temperature roasting [29]. The roasted product is cooled to room temperature, ground to finer sizes, and then leached out with water or acid. The experimental conditions, predominantly roasting temperature and time, depend on the nature of additives used. In most cases, it has been possible to extract 90-95% of potassium from feldspar/other potassium-bearing minerals at 800-1,100 °C with 1-2 h of roasting time [27,30-32]. Recently, microwave-assisted heating methods have been reported for potassium extraction from nepheline syenite [22]. Also, there are reports regarding the use of low dosages of sodium fluoride as roasting additive for potash recovery from pyrophyllite mine waste with a very low roasting time [33]. Some of the important examples of potassium extraction from feldspar or similar minerals using the roast-leach method and the experimental conditions reported in the literature are shown in Table 1. The extraction of such high potassium values during roasting can be attributed to the collapse of feldspar lattice structure. As shown in Table 1, among all such additives, roasting with $CaCl_2$ alone or in combination with NaCl always provides better results than other reported additives. The use of $CaCl_2$ and NaCl is also preferred because of their low cost and environment-friendly nature in comparison to other groups (I-A and II-A) of metal chlorides such as $SrCl_2$, $BaCl_2$, $RaCl_2$, and LiCl.

In continuation of our earlier attempts to extract potassium [21, 22,26,33], this study was undertaken to extract potassium using $CaCl_2$ and NaCl independently as additives from feldspar and to investigate the kinetics and mechanism of the extraction process. The major experimental factors such as particle size, roasting temperature, roasting time, amounts of additives, and leaching conditions of roasted masses were optimized. Although in both the cases, soluble sylvite mineral (KCl) was formed, $CaCl_2$ was found to be a better roasting additive for potassium extraction. This difference in extraction efficiency between the two additives has been elucidated.

MATERIALS AND METHOD

1. Materials

1-1. Chemicals

The additives, sodium chloride, calcium chloride were obtained from Central Drug House (P) Ltd, New Delhi and analytical grade with high purity (99.8%). The other chemicals used in the process were supplied by Avantor Performance Materials India Limited, Gurgaon and all were of analytical grade reagents with a purity of approximately 99.8%.



Fig. 1. The collected feldspar sample.

1-2. Mineral Sample

The feldspar ($KAlSi_3O_8$) sample was obtained from Rajasthan state in India. A photograph of the as-received sample is shown in Fig. 1. The sample appeared brownish with sporadically distributed light blue and black patches throughout its surface. It was fragile and soft to touch.

The size reduction of the as-received sample was carried out by using a laboratory jaw crusher (Eastman Crushers Company Pvt. ltd., Kolkata-India) followed by roll crusher (Rajco Science and Engineering Products, New Delhi-India) and finally, in a ball mill (Kaycee Industries Ltd, Bombay-India) to get the fine materials for different roasting studies. The ball mill grinding was carried out at different intervals of time and the product was subjected to size analysis at the end of grinding using standard sieves.

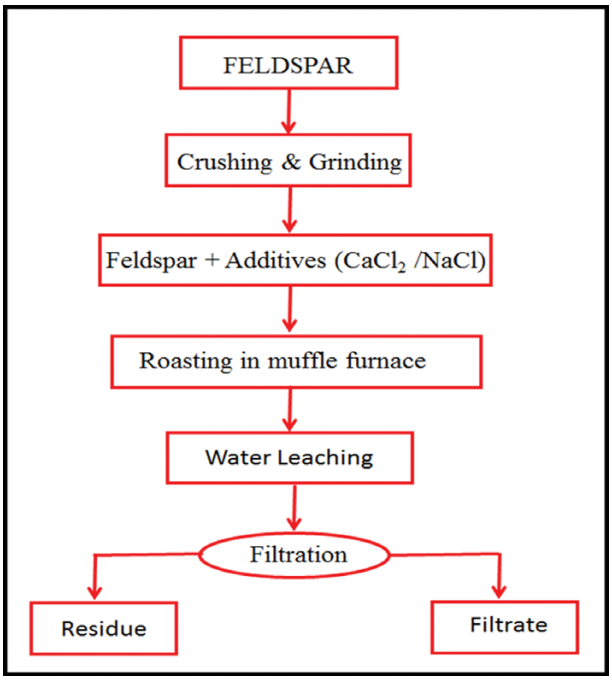
2. Characterization

The systronic flame photometer (Model 128 μC), ICP-OES (Optima 8300, Perkin Elmer), and standard wet chemical analysis methods were used to determine the elemental composition of the sample. The X-ray diffraction (XRD) measurements of the powdered sample were performed by Rigaku X-Ray diffractometer using

a Cu-Kα irradiation source. The morphology and surface composition of the feldspar feed, roasted and roast leached samples were studied by scanning electron microscope (SEM, Zeiss Make) equipped with energy dispersion spectroscopy. Samples were analyzed as loose powders on carbon stubs taken after coating with Au-Pd to dismiss the charging effect. The FTIR spectra of the samples were recorded on a Perkin Elmer Spectrum GX model instrument in the range of 400-4,000 cm^{-1} over a KBr disc pellet. The KBr disc was made up of a thorough mixture of 2 mg of samples with 100 mg KBr. The disc was initially evacuated for 5 min followed by a pressure of 5 tons. The Raman spectra of the bulk, roasted and roast-leach residue of feldspar were obtained using a Renishaw inVia Raman microscope, with a 514 nm excitation wavelength of an Ar ion laser. The powdered sample was placed under the microscope using the 50X objective lens.

3. Methods: Roasting and Leaching

The roasting studies were carried out in a laboratory muffle furnace (Therelek Furnaces Private Ltd, Thane-India, Operating temperature 1,200 °C in air, ramp rate 6 °C/min) having digital temperature and time controller. The sample was mixed carefully with either NaCl or $CaCl_2$ in a silica crucible and then roasted at the pre-set temperature and time. The weight percentage of the roasting additives was taken with respect to the weight of feldspar during the roasting process. After roasting the sample was taken out of the furnace and cooled at room temperature. The resultant fused mass was broken into small pieces by a hand mortar to ensure effective leaching. The water leaching studies were carried out in a glass beaker by varying the solid: liquid ratio, temperature, time and stirring speed of the agitator. Ultimately, the leached solution was filtered through a Whatman 41 filter paper. The residue was washed for 5-6 times repeatedly for entire partitioning of the water soluble chlorides formed during roasting. The experiments were repeated at least three times for ascertaining the reproducibility of the result. The average values were taken and the standard error was found to be within ±0.2%. The overall extraction process of potassium from feldspar and the experimental parameters is depicted in Scheme 1 and Table 2 respectively.



Scheme 1. Flow sheet for potassium extraction from feldspar.

Table 2. Experimental parameters for roasting and leaching studies

Roasting conditions		Leaching conditions	
Particle size (μm)	38-500	Temperature (in °C)	30-95
%, NaCl (w/w)	25-200	Time (in min)	10-60
%, $CaCl_2$ (w/w)	25-200	%, Solid	5-40
Temperature (in °C)	700-950	Stirring speed (RPM)	600
Time (in min)	5-60		
Cooling time (in min)	60		

The percentage of potassium value extracted from the feldspar is calculated by using Eq. (1).

$$f=\left[1-\frac{C_1}{C_2}\right]\times 100 \quad (1)$$

where C_1=percentage K_2O in roast-leached residue with respect to the mass of feldspar; C_2=percentage K_2O in bulk feldspar sample.

RESULTS AND DISCUSSION

1. Characterization of Feed Sample

1-1. Chemical Analysis

The chemical analysis of the feldspar sample was by both wet chemical and instrumental methods (ICP-OES and Flame photometer). The results are presented in Table 3. The finely ground (<100 μm) dried sample (~1 g) was digested in a Teflon beaker using hydrofluoric acid (10 ml) and nitric acid (5 ml) over a digitally controlled hot plate. It was heated to dryness till evaporation of all the added acids. Then 20 ml of 1 : 1 diluted HCl was added and again heated for 15 min to redissolve the dried mass. After that the solution was filtered to a volumetric flask and diluted further, if necessary for analysis. The mother liquor was used to determine the iron and alumina content of feldspar by wet chemical methods, and the silica content was calculated gravimetrically following the Bureau of Indian Standards (BIS) procedure. However, the other components like Na, K, Ca, and Mg were determined from the same mother liquor using flame photometer and ICP-OES. Certified standards were simultaneously analyzed in order to

Table 3. Chemical analysis of the Feldspar sample

Constituents	Percentage (%)
K_2O	11.64
Na_2O	3.03
Fe_2O_3	0.79
CaO	0.54
MgO	0.39
Al_2O_3	16.29
SiO_2	66.82
LOI	0.22

ascertain the analysis results. The loss on ignition (LOI) of the sample was carried out after igniting a known weight of sample in a muffle furnace at 950 °C as per Indian standard specifications. This analysis data reveals that K_2O, Al_2O_3, and SiO_2 constituted more than 94% of the total composition. The loss on ignition (LOI) was very low, which indicates the absence of free moisture or hydroxyl bearing groups within the crystal structure of feldspar sample.

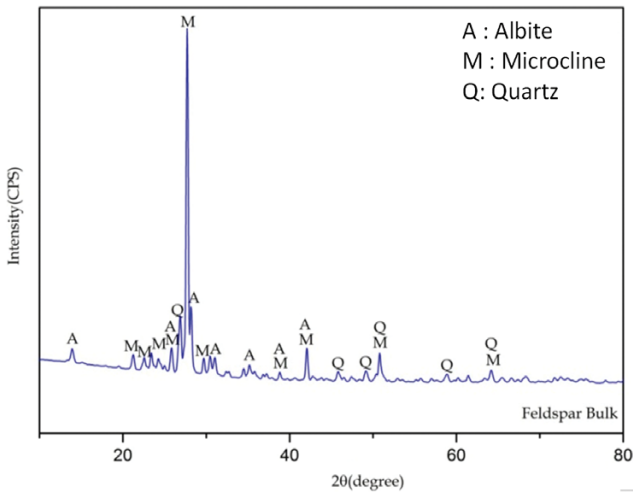


Fig. 2. XRD patterns of feldspar sample.

1-2. Mineralogical Composition Analysis

The mineralogical compositions of the feed feldspar sample were analyzed from X-ray diffraction pattern, SEM-EDS and elemental mappings. The X-ray diffraction pattern of the feed sample is presented in Fig. 2. It is indicated from the figure that microcline mineral occurs as the major phase with albite and quartz in minor amount.

The sodium content in the sample is attributed to albite phase, whereas microcline phase is the major possessor of potassium. The mineral phases were further confirmed through SEM-EDS analysis as shown in Fig. 3. The electron micrograph and their semi-quantitative elemental analyses illustrate the presence of silicate minerals along with Al, K and a meagre amount of Na in the feed feldspar sample (Fig. 3). The elemental mappings of the feed sample envisage the occurrence of both sodium- and potassium-bearing aluminium silicate phases. From the micrograph, the feldspar minerals are found to be composed of elongated and granular forms of various phases like albite, orthoclase and microcline. The ele-

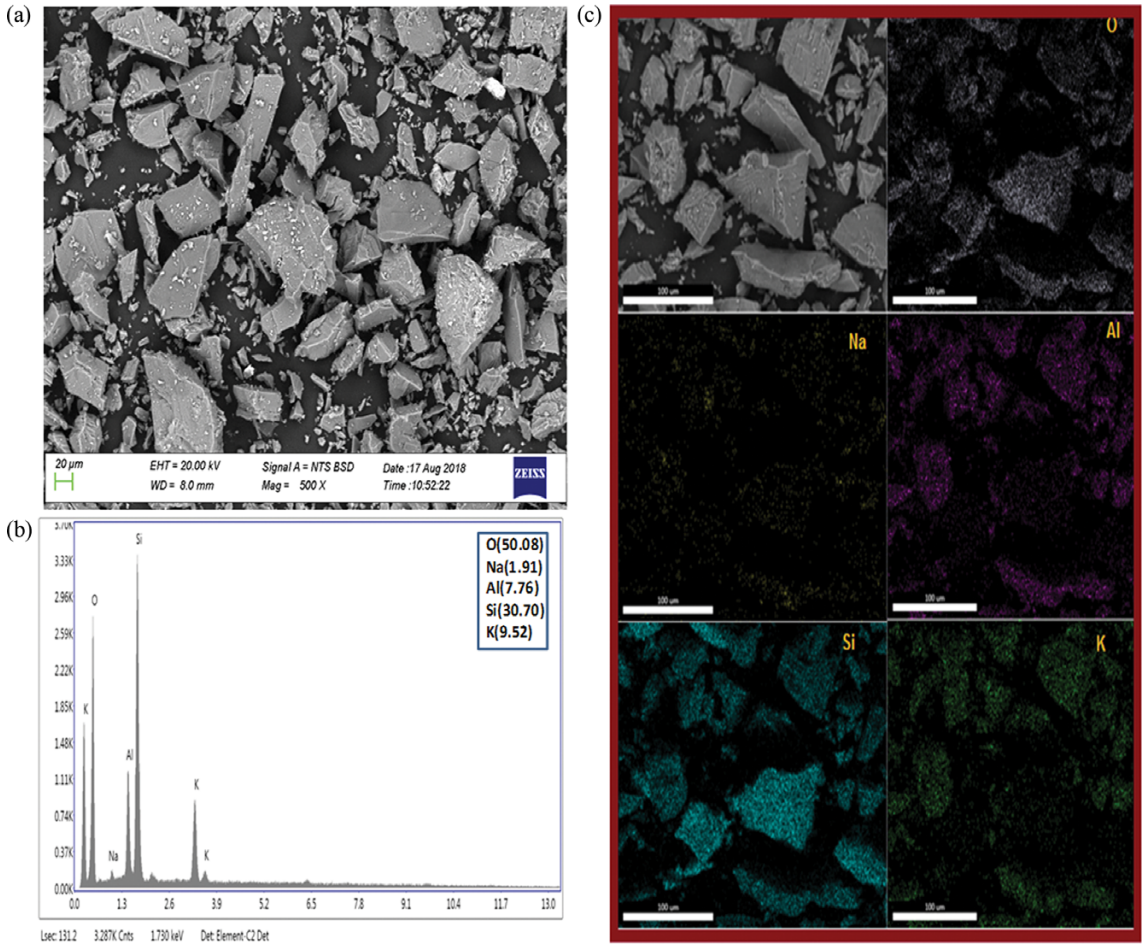


Fig. 3. SEM-BSE image showing the presence of Na, Al, Si, K and O in the feed sample confirming the presence of albite and microcline ((a), (b)); Compositional mapping of feldspar sample showing the distribution of different elements (1st is the BSE image, (c)).

mental distribution of different phases indicates that albite and orthoclase/microcline are the feldspar group of minerals present in the feed sample. The potassium is found in orthoclase and microcline whereas sodium is present in albite.

2. Batch Studies

2-1. Effect of Grinding

In the selection of a suitable size of mineral for efficient extraction, the sample was subjected to the ball mill grinding at different intervals of time and subsequent size analysis through different sieves. The particle size distribution analysis of the sample is demonstrated in Fig. 4(a). As seen from the plot, the weight percentage of 80% passing sizes (d80) continues to increase with increase of grinding time and the size of the particle also reduces with time. At time intervals of 15, 30, 45 and 60 min the sizes were determined to be 85, 66, 38 and 34 microns (μm), respectively. Further, it is observed that change in particles size is almost negligible beyond 45 min of grinding (Table 4). The ground products obtained after each grinding time were subjected to chemical analysis by wet chemi-

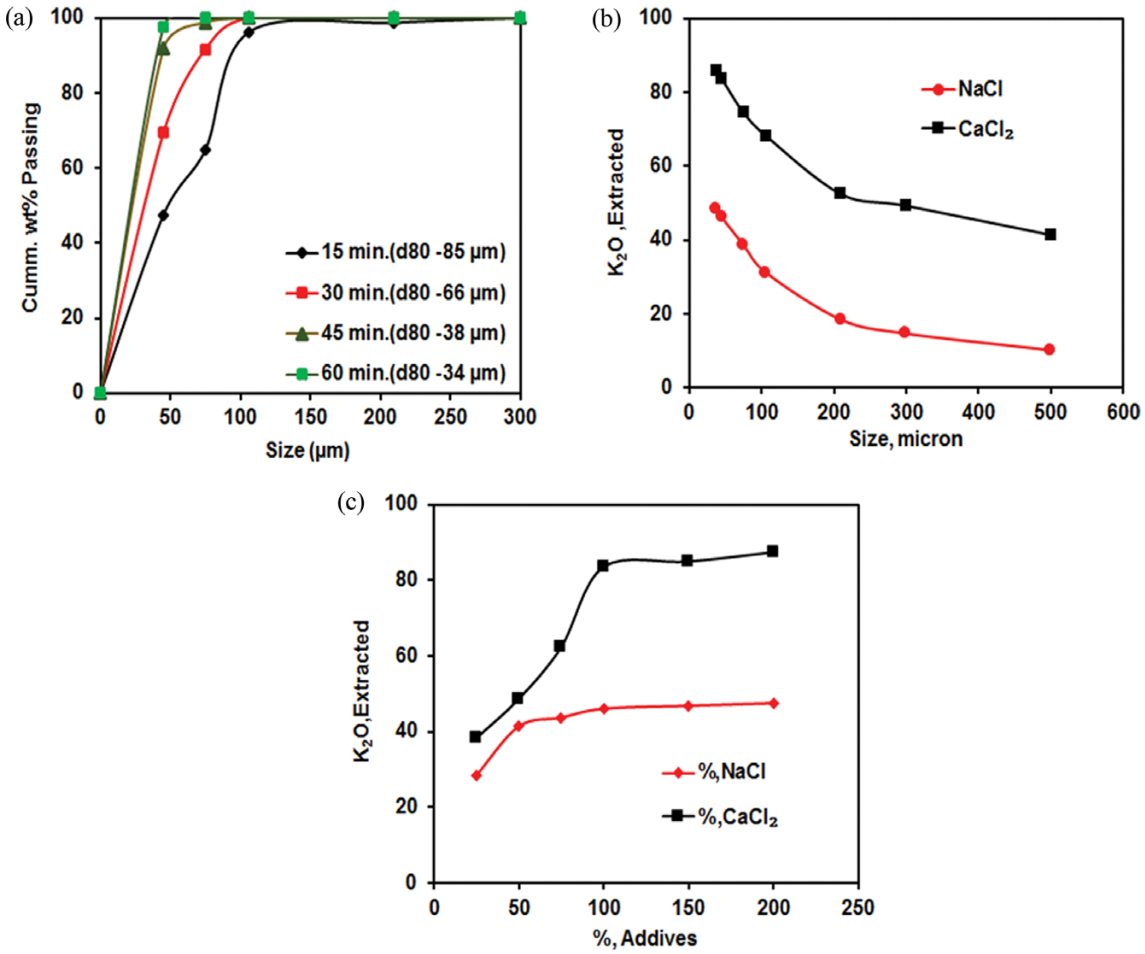


Fig. 4. Batch studies: (a) Size analysis of the ball mill ground products; (b) Effect of particle size for potash recovery; (c) Effect of roasting additives on potash recovery.

Table 4. Chemical analysis of the ball-mill ground feldspar products

Size, μm	15 min (d80, 85 μm)		30 min (d80, 66 μm)		45 min (d80, 38 μm)		60 min (d80, 34 μm)	
	Cum. wt%	K_2O, %	Cum. wt%	K_2O, %	Cum. wt%	K_2O, %	Cum. wt%	K_2O, %
−500+300	100	11.01	100	10.89	100	11.12	100	11.09
−300+210	98.8	11.20	100	11.02	100	11.32	100	10.98
−210+106	96.3	11.26	100	11.35	100	11.24	100	11.31
−106+75	64.9	11.39	91.7	11.52	98.8	11.72	100	11.21
−75+45	47.5	11.52	69.4	11.60	91.8	11.65	97.6	11.62
−45	33.9	11.84	50	11.75	73.8	11.69	84.1	11.77

*μm: micron

cal method to determine the potassium values content in the fraction. On analyzing the data it is revealed that the amount of potassium values recovered was around 11% in all cases irrespective of particle size. These observations support two following issues: (i) potassium is distributed throughout the feed mineral homogeneously, and (ii) the additional increase in the liberated potassium did not occur even after grinding to the finer sizes possibly because of the entrapment of potassium (in K^+ form) within the complex three-dimensional framework of feldspar. Potassium may be linked through SiO_4 and AlO_4 tetrahedra to preserve the electrical neutrality of the system. Thus, for unlocking the potassium from Al-O-Si and/or Si-O-Si network, it is necessary to demolish the crystal lattice of feldspar as much as possible. The roasting with selective additives followed by leaching with water could the best possible method to ensure complete recovery of potassium values from feldspar.

2-2. Effect of Particle Size

The effect of particle size on the recovery of potash was studied in the presence of two additives: NaCl, and $CaCl_2$ individually. The particle size was varied from 38 μm to 500 μm taking feldspar : additive in 1 : 1 ratio, roasting temperature 900 °C, and roasting time 60 min. The roasted product thus obtained was leached with water for 15 min at room temperature. The results are in Fig. 4(b). It is clearly illustrated by the figure that with a decrease of particle size from 500 μm to 38 μm in the presence of both the additives, the potassium recovery increases. The increase in surface area due to decrease in particle size enhances additive-feldspar contact effectively, which in turn enhances the extent of the potassium recovery. The effect of particle size as presented in Fig. 4(b) for both the additives $CaCl_2$ and NaCl indicates a higher recovery using $CaCl_2$, and this is due to many factors like charge of cations, size of cations, and electronegativity of Si/O as discussed in Section 3.3 (Mechanism of potash recovery). However, marginal change in recovery on reducing the particle size from 45 μm to 38 μm was observed; this suggests the limiting effect of particle size on the liberation of potassium mineral. Therefore, further experiments were carried out taking particle size of 45 μm.

2-3. Effect of Roasting Additives

The effects of weight percentage of both the additives (NaCl and $CaCl_2$) with respect to feldspar on the potash recovery were studied maintaining the roasting temperature, time and particle size of feldspar at 900 °C, 60 min and −45 μm, respectively. Each time the roasted products were leached in water for 15 min. The recovery results are presented in Fig. 4(c). As is observed from the plot, potassium recovery increases with increase of additive in presence of both the additives till a plateau is reached. However, $CaCl_2$ could recover 86% of potash whereas NaCl could recover only 44% under the same experimental conditions. The maximum recovery in case of NaCl was accomplished when additive percentage was 50%. With further increase of the percentage of additive, there was no significant effect on the recovery of potash. On the contrary, in presence of $CaCl_2$ the potassium recovery continuously increased with increase of additive percentage up to 100% with respect to feldspar weight; the recovery percentage did not change significantly on increasing the percentage of additive further. This result may be attributed to the difference in the electrical charge of the balancing ions. Theoretically, a calcium atom with two positive charges can effectively replace two potassium ions in the crystal lattice, whereas univalent sodium ion can replace only one potassium ion [33].

3. Mechanism of Potash Recovery

Feldspars are tectosilicate minerals consisting of three end members: K-feldspar ($KAlSi_3O_8$), albite ($NaAlSi_3O_8$) and anorthite ($CaAl_2Si_2O_8$). Alkali feldspars are solid solutions of albite and K-feldspar, whereas plagioclase is the solid solution of albite and anorthite. Feldspar consists of a three-dimensional network of interconnected tetrahedra of O, Al and Si atoms in which each Al atom is bonded to four tetrahedrally arranged oxygen atoms. This arrangement therefore, requires one unit of residual positive charge to be balanced (Fig. 5).

The positively charged K, Na, Ca ions etc. are entangled in this network to provide electrical neutrality to the mineral [47,48]. In orthoclase, this deficiency of electron is fulfilled by K atom (which, therefore, becomes K^+), whereas in albite and anorthite the electrical neutrality of the crystal is achieved by Na and Ca, respectively. Possibly because of this reason, the leaching of potassium from feldspar with the help of inorganic acids is low [29,37]. Thus, in

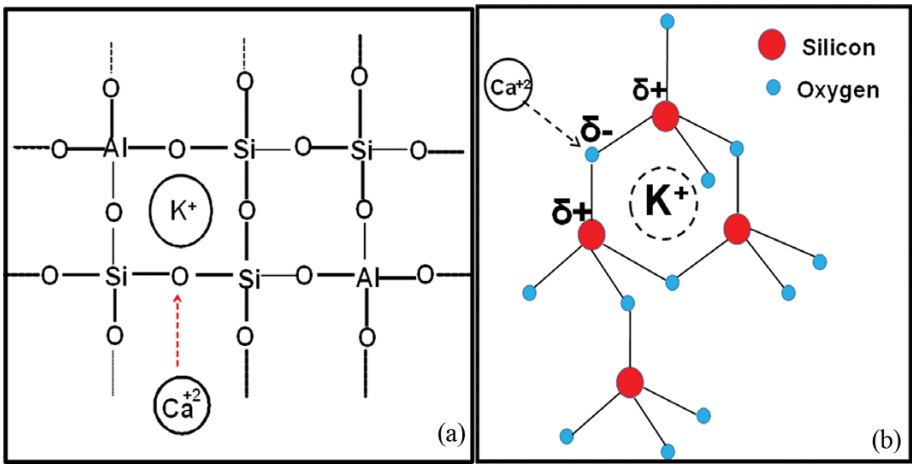


Fig. 5. (a) Localization of K^+ in the crystal matrix of feldspar, (b) Suitable orientation of Ca^{2+} ion during the replacement of K^+ ion of feldspar.

order to release K atom from this network the crystal structure of feldspar needs to be broken. The isomorphic replacement of potassium (K^+) with sodium (Na^+) or calcium (Ca^{+2}) ions can also facilitate potassium release from the three-dimensional network of feldspar. However, this replacement is facilitated only at high temperature, i.e., above 750 °C [33] as both the additives are high melting compounds. Consequently, as a rule, roasting methods using chloride salts of alkali and alkaline metal ions are preferred to leaching (acid/alkali leaching) methods.

Both the salts (NaCl and $CaCl_2$) can react with feldspar at a high temperature to bring potassium into soluble form, i.e., sylvite (Potassium chloride) [34]. The other salts of group IA and IIA like LiCl, $SrCl_2$, $BaCl_2$, and $RaCl_2$ are not preferred as these are highly expensive, radioactive and environmentally deplorable as well. Though the mechanism shown above explains the formation of sylvite in both the cases during roasting, $CaCl_2$ yields maximum potash via this route. Eqs. (2)-(5) represent the possible chemical reactions occurring between the K-bearing silicates with $CaCl_2$ and NaCl during roasting process [32,33]. Accordingly, calcium aluminium silicate (anorthite), sylvite (KCl), halite, albite and quartz etc. are formed on roasting in presence of these two salts.

$$2KAlSi_3O_8+CaCl_2\rightarrow 2KCl+4SiO_2+CaAl_2Si_2O_8 \quad (2)$$

$$2NaAlSi_3O_8+CaCl_2\rightarrow 2NaCl+4SiO_2+CaAl_2Si_2O_8 \quad (3)$$

$$KAlSi_3O_8+NaCl\rightarrow KCl+2SiO_2+NaAlSiO_4 \quad (4)$$

$$2SiO_2+NaAlSiO_4\rightarrow NaAlSi_3O_8 \quad (5)$$

The mutual ion exchange between K^+ and Ca^{2+} could be possible within the crystal matrix as these two ions are isoelectronic with each other, whereas this may not be that favorable with Na^+ ion (Supplemental Table S1). Further, relatively greater ionic radius of Ca^{2+} (0.99 A°) may be a better replacement for K^+ (1.33 A°) within the crystal lattice in comparison to Na^+ (0.95 A°) [38]. Since K^+ acts as a charge balancing ion in the crystal lattice of feldspar, for everyone Ca^{2+} ions, two potassium ions are released during the extraction process. On the contrary, water-soluble sodium silicate is formed in presence of NaCl due to the reduction of feldspar, which may increase the viscosity of the solution and, therefore, may obstruct the breakdown of crystal structure in comparison to $CaCl_2$. Thus, the higher valency and larger non-hydrated ionic radii of Ca^{2+} reinforce its candidature as a superior replacement in comparison to Na^+ ion, resulting in higher cation replaceability factor of $CaCl_2$ with respect to NaCl. The formation of KCl and its release are also evident considering the electronegativity difference and lattice energy of formation values (Supplemental Table S1). The possible chlorides that may be formed during the roasting process are KCl, NaCl, $AlCl_3$, and $SiCl_4$. Since the electronegativity difference between Cl and X (where X is K or Na or Al or Si) is highest (2.18) in the case of KCl and lattice energy for the formation of KCl is lowest in comparison to others, the formation of KCl is more probable. $SiCl_4$ is volatile and formation of $AlCl_3$ can be ignored as aluminium (Al^{3+}) being in +3 valence state its replacement by Ca^{2+}/Na^+ in the crystal structure may not be possible. The mechanism as depicted in Fig. 5 reveals that, in the two-dimensional diagram of a feldspar unit, every fourth tetrahedral unit of SiO_4 contains an aluminum ion at its center. It is known that the bridging oxygen atom is slightly negatively charged (electronegativity value 3.5) and the bonded silicon atoms are slightly positively charged (electronegativity value 1.7). Thus, because of this dipositivity nature, Ca^{2+} ions can be adsorbed faster onto crystal surface of feldspar compared to Na^+. The partial bonding of calcium ion with the bridging oxygen atom of the feldspar introduces a strain in Si-O bond, thereby weakening the bond. Consequently, the

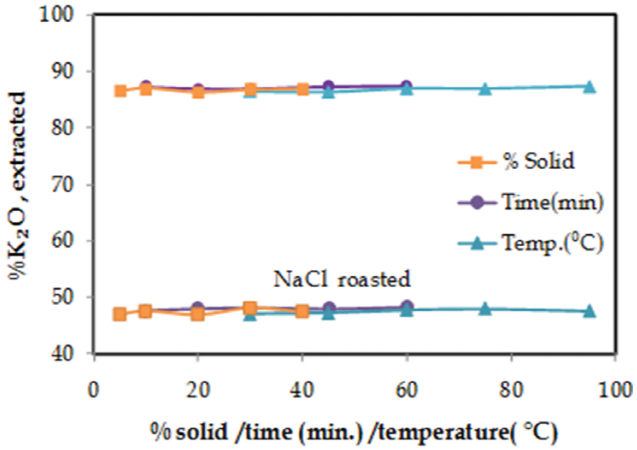


Fig. 6. Water leaching study of roasted feldspar.

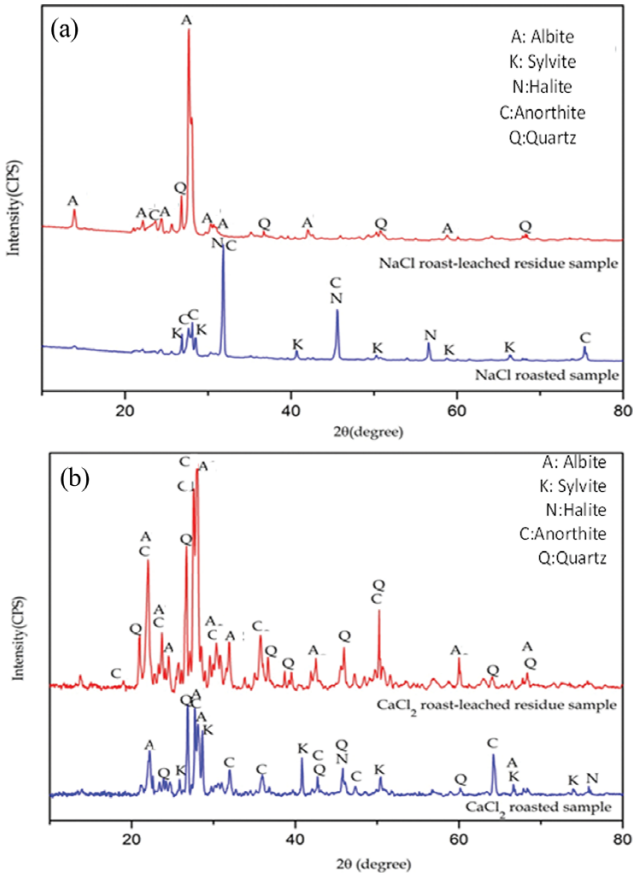


Fig. 7. XRD patterns of (a) NaCl roasted and roast-leached products and (b) $CaCl_2$ roasted and roast-leached products.

approach of Ca^{2+} ions towards the lattice center becomes easier in order to replace the K^+ ion from the crystal structure. The released potassium ion also becomes stable due to the formation of sylvite minerals.

4. Water Leaching Study

Experimental parameters like percentage of solid, leaching temperature, stirring speed of the digital agitator and leaching time were studied to optimize the leaching efficiency of roasted products. The roasted mass was generated by taking a fixed ratio of feldspar to additives in 1 : 1, the roasting temperature and roasting time as 900 °C and 60 min, respectively. The effects of experimental factors were observed by varying one parameter at a time while keeping the rest of the parameters constant (Supplementary Table S2). The results are demonstrated in Fig. 6 which clearly manifests that the leaching efficiency of potassium ions from the roasted mass is independent of the variation of the parameters. This suggests that formation of sylvite mineral during the roasting process is the determining step for potassium extraction. Once this is formed, the leaching takes place instantaneously.

5. Product Analyses

5-1. X-ray Diffraction and SEM Studies

X-ray diffraction (XRD) studies of both the roasted and roast-leached products were conducted to support the formation of sylvite as illustrated in Fig. 7. The different mineral phases formed during roasting followed by leaching, i.e., roasted and roast-leached residue, were identified from the positions of various peaks. The appearance of sylvite mineral in the roasted product and its disappearance in the leached products support the isomorphic substitution of K with Na or Ca. Since calcium-rich mineral anorthite ($CaAl_2Si_2O_8$) formed as the roasted product is water insoluble [39], its peaks are also detected in the XRD spectra of roast-leached residues. The peak of halite (NaCl) in roasted product after water leaching could not be detected because of its water solubility.

SEM studies of the roast- leached products using both the additives are presented in Figs. 8 and 9. A significant difference of leached products was already observed from its bulk sample (Figs. 2 and 3). The bulk feldspar sample after roasting becomes a hard-uniform mass with faint brownish-white color, whereas after leaching it becomes dull white with a soft feel. As seen from the BSE image, the dense structure of roasted feldspar product is due to the agglomeration of feldspar particles occurring as a result of the reactions with melting additives, $CaCl_2$ and NaCl.

The deformation of particle sizes (Fig. 8(a), 9(a)) may be due to the occurrence of solid-state chemical reactions. The diminution of the agglomeration of particles (Fig. 10) and resulting sparkling surfaces of dispersed particles is due to the dissolution of sylvite formed during roasting and high water-soluble nature of unreacted melted NaCl or $CaCl_2$ (if any) present during the roasting process. Fig. 10(b) represents the formation of anorthite (elongated shape) along with a little sylvite in exsolved state. The semi-quantitative

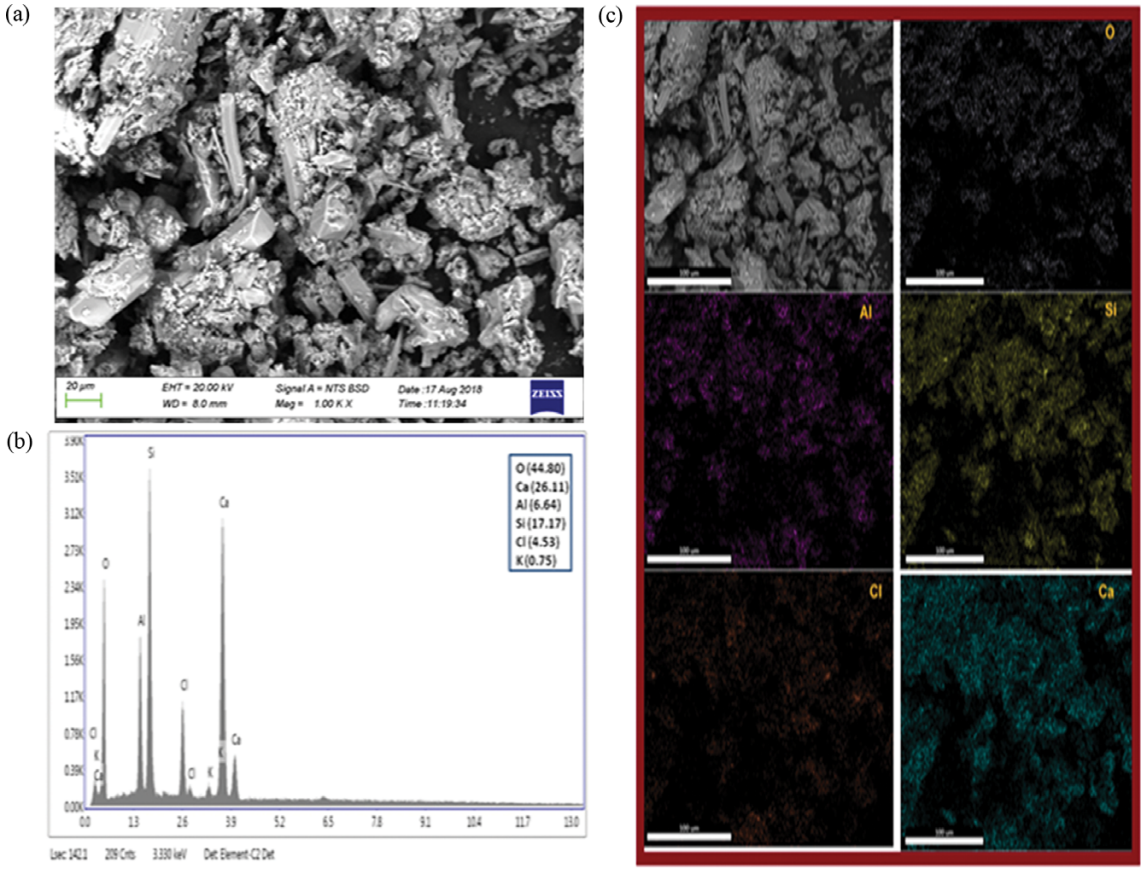


Fig. 8. SEM-BSE image showing the presence of Ca, Cl Al, Si, and O in the $CaCl_2$ roast-leached sample ((a) & (b)). Compositional mapping of $CaCl_2$ roast-leached sample showing the distribution of different elements (1st is the BSE image) (c).

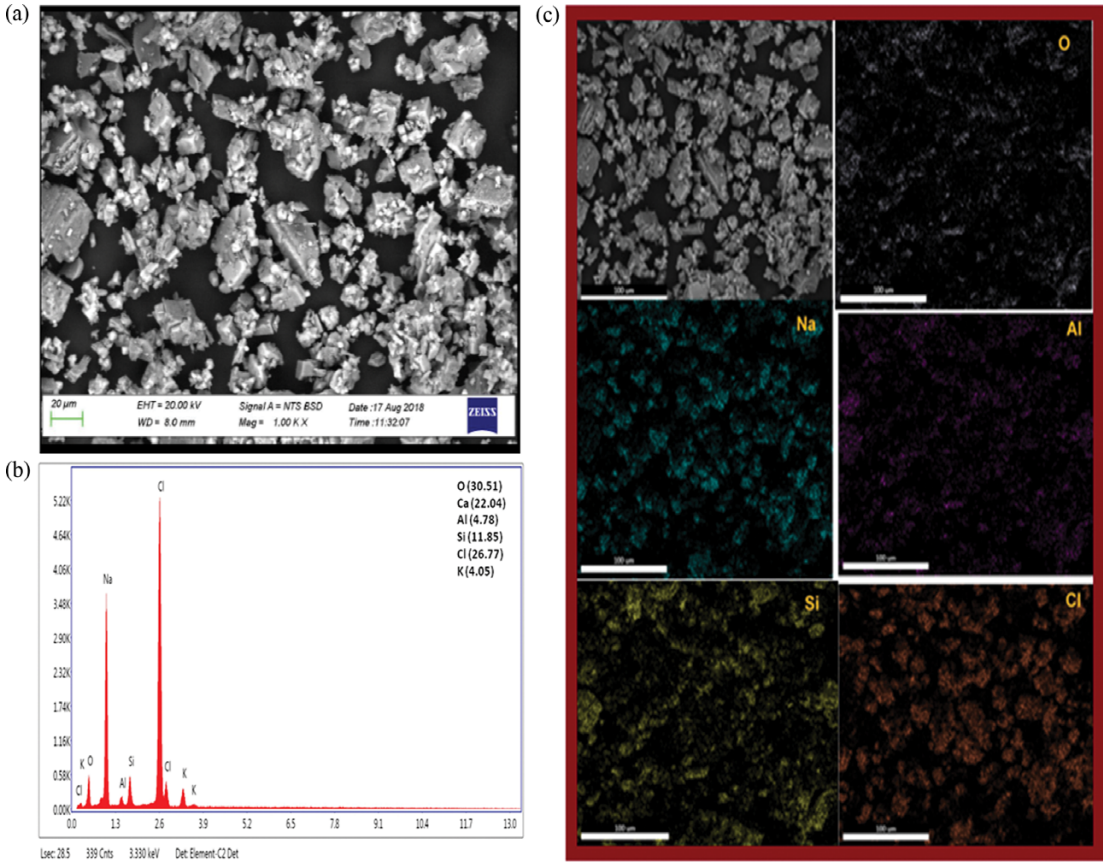


Fig. 9. SEM-BSE image showing the presence of Na, Al, Si, Cl, K and O in the NaCl roast-leached sample ((a), (b)); Compositional mapping of NaCl roasted sample showing the distribution of different elements (1st is the BSE image) (c).

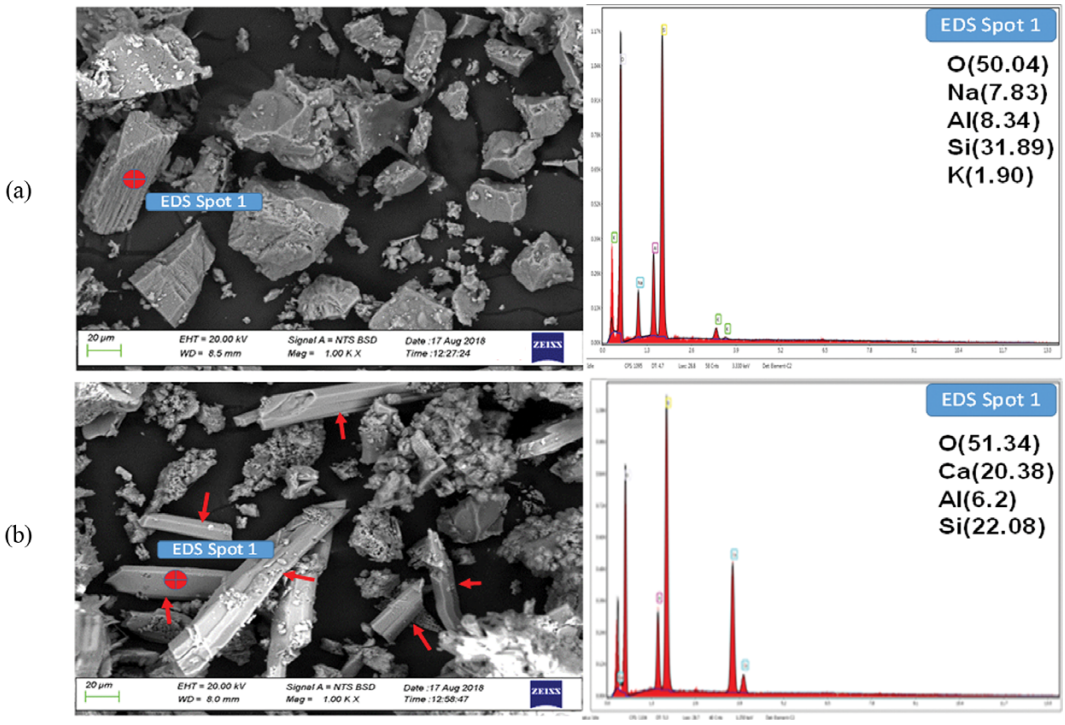


Fig. 10. (a) SEM-BSE image of the NaCl roast-leached sample and the compositional mapping showing the distribution of different elements. (b) SEM-BSE image of the $CaCl_2$ roast-leached sample and the compositional mapping showing the distribution of Ca, Al, Si, and O.

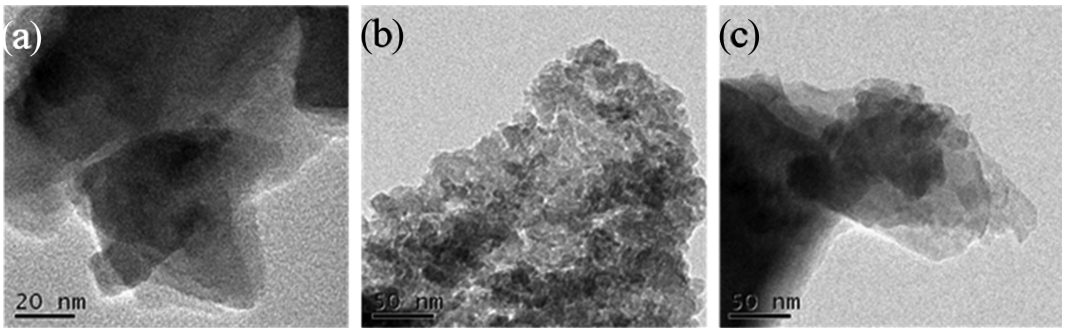


Fig. 11. TEM images of the (a) bulk feldspar (b) $CaCl_2$ roasted mass (c) NaCl roasted mass.

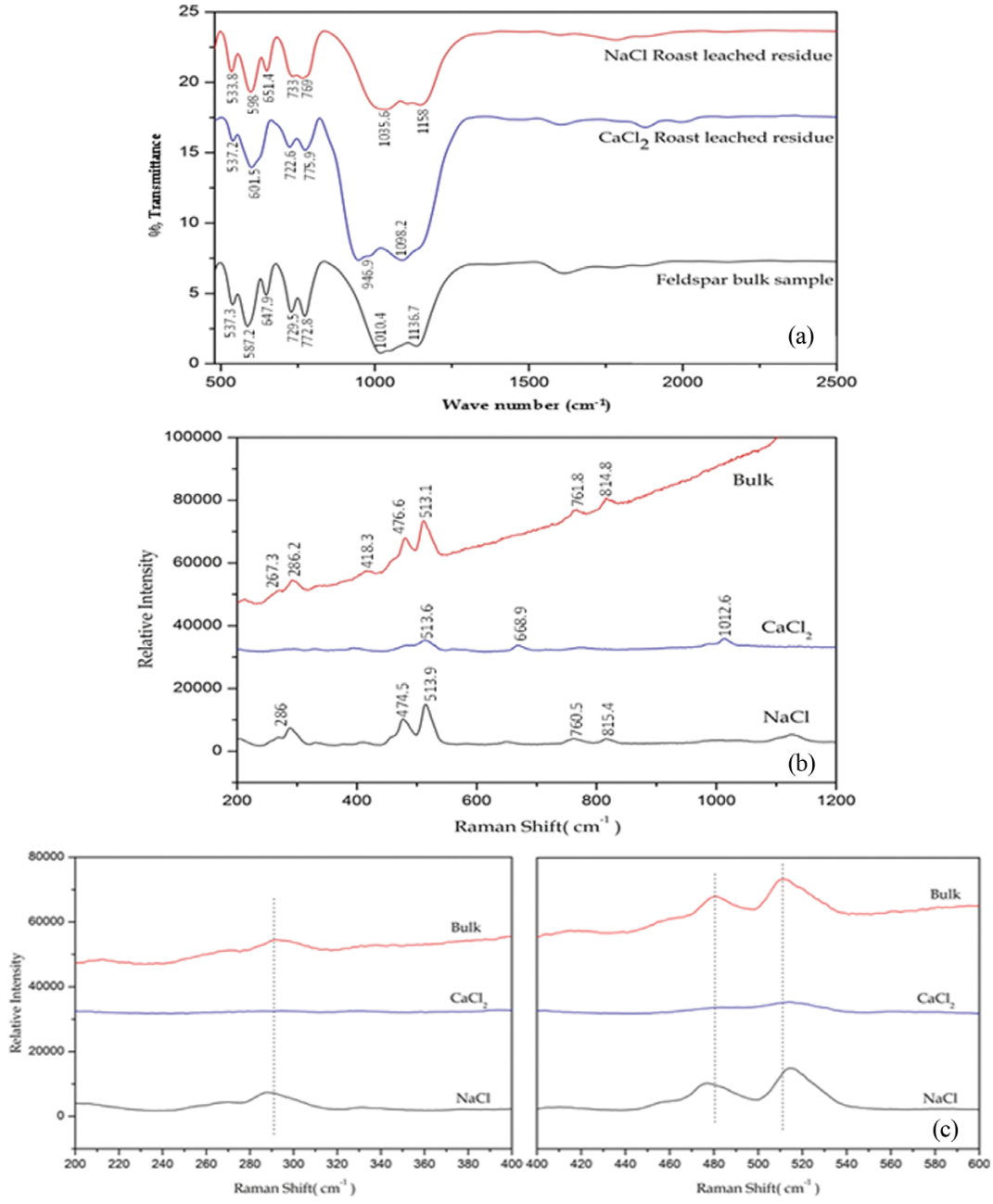


Fig. 12. (a) FTIR spectra of bulk and roast - leached feldspar residues; (b) Raman spectra of bulk and roasted feldspar product; (c) Magnified Raman spectra of bulk and roasted feldspar product (Raman shift 200-400 cm^{-1} and 400-600 cm^{-1}.

observations confirm the presence of Ca-aluminium silicate (Anorthite), whereas the K and Cl content contribute towards the presence of sylvite in the roasted sample. The formation of euhedral hexagonal crystals of anorthite during $CaCl_2$ roasting and disappearance of sylvite after water leaching is clearly discernible during the process of extraction. The adjacent semi-quantitative data along with the EDS suggest the sample to be rich in anorthite after leaching of the roasted product. However, when the feldspar samples are subjected to roasting with NaCl, anorthite is formed with sylvite and halite and after leaching the formation of albite is greater than anorthite (Fig. 10(a)). A small amount of quartz is also formed. The leached products are seen to be rich in albite (Na-bearing Al-silicate) with little potassium in their crystal lattice as separated grains.

5-2. Transmission Electron Microscopy (TEM)

TEM analyses of the bulk and roasted samples are shown in Fig. 11. Similar morphology in TEM is manifested as obtained in SEM. Bulk feldspar samples are roasted at high temperature in the presence of both the additives independently. The bulk feldspar sample shows hard mass as shown in Fig. 11(a). In the presence of additives such as $CaCl_2$ and NaCl the roasted feldspar got agglomerated as manifested in Fig. 11(b) and Fig. 11(c). The deformation of particle sizes may be due to the occurrence of solid-state chemical reactions.

5-3. FTIR and Raman Spectra Studies

FTIR analyses were performed to identify the changes in chemical structure of feldspar during the roast-leach technique. The overlay spectra of the product and feed materials are provided in Fig. 12. In the mid-FTIR spectral region (400-1,400 cm^{-1}) the peaks corresponding to the vibrations of Si and Al bonds with respect to O atom in the feldspar structure (Si-O, Si-O-Si, Si-O-Al, etc.) are identified. In the spectral region between 1,000-1,200 cm^{-1} two broad bands are observed at 1,010.4 cm^{-1} and 1,136.7 cm^{-1}. The various bands obtained in the feldspar, $CaCl_2$ roast-leached residue, NaCl roast-leached residues are summarized in Supplementary Table S3. The FTIR spectra and the data collected from literature indicate that chemical/physical changes occur in the bulk, roasted and roast-leached residue during the recovery process. Physical observation and comparison show that all the three products (bulk, roasted and roast-leached residue) are different from each other.

The analyses of the FTIR peaks (Fig. 12(a), supplementary Table S3) confirm the breakdown of feldspar structure and formation of new secondary minerals during roasting. The presence of four band positions at 573.3, 647.9, 1,010.4 and 1,136.7 cm^{-1} indicates the presence of microcline in the bulk feldspar sample, whereas the presence of band positions at 1,098.2 cm^{-1} (for $CaCl_2$ roast-leached residue) and at 1,035.6, 1,158 cm^{-1} (for NaCl roast-leached residue) confirms the presence of albite mineral [40,41]. The peak at 647.9 cm^{-1} in bulk feldspar is due to O-Si (Al)-O bending vibrations of microcline, which is completely disappeared in $CaCl_2$ roast leached residue, indicating the breaking of O-Si (Al)-O bond in the crystal structure [42]. Some peaks completely disappear with evolution of some other new peaks due to changes in the crystal structure of feldspar. All these FTIR data support the physical or chemical changes in the crystal structure of the feldspar after roasting and leaching. As is evident, the peaks observed in the bulk feldspar ore are partially or completely different from the roast-leached residue.

The Raman spectra (Fig. 12(b)) of the bulk sample with the roasted and the roast-leached residue exhibit seven major peaks in the bulk feldspar sample, whereas five and eight in the case of $CaCl_2$ and NaCl roast-leached products, respectively. The two major peaks obtained in the 450-520 cm^{-1} spectral region belong to the ring-breathing modes of the four member rings of tetrahedron. Peaks in the range of 200-400 cm^{-1} are due to the rotation translational modes of the ring and below 200 cm^{-1} is for cage shear modes of the ring. The peaks in the spectral region of 900-1,200 cm^{-1} are assigned for vibration stretching modes of the tetrahedral structure. The two major peaks for bulk feldspar at 513.1 and 476.6 cm^{-1} are due to the ring-breathing modes of the four member rings of tetrahedra (TO_4), and the other two peaks at 286.2 and 267.3 cm^{-1} are due to the tetrahedral rotational-transitional modes, which supports the presence of microcline as the major K-feldspar mineral in the ore [43-45]. In the spectral region of 400-600 cm^{-1}, the $CaCl_2$ product gives a very low-intensity band width peak (at 513 cm^{-1}), whereas the peaks for NaCl roasted product are slightly disturbed in comparison to the bulk ore. The relative intensities of peaks in the case of $CaCl_2$ roasted sample are less than that of the bulk ore, indicating the disappearance of tetrahedral rings in case of the $CaCl_2$ roast-leached residue. Fig. 12(c) compares the bulk and roasted products. The $CaCl_2$ roast-leach residue spectrum does not show any remarkable peak, indicating the destruction of four-membered tetrahedral rings during the roasting event as a result of which the release of potassium is maximized. On the other hand, the shifting of peaks in NaCl roasted-leached sample, lower frequency region, indicates the formation of anorthite [43,44].

6. Kinetics of Potash Recovery

The validity of various kinetic models for analyzing the solid-state reactions for potash recovery from feldspar was established by assuming the spherical geometries of the particles [46]. The movement of reaction may be controlled by either of the following ways. If the reaction is controlled by the interface, the integrated rate equation can be expressed as given in Eq. (6),

$$1-(1-f)^{1/3}=k_1t \quad (6)$$

Or, if the reaction is controlled by diffusion at the product layer, the integrated rate equation can be expressed as given in Eqs. (7)-(8),

$$[1-(1-f)^{1/3}]^2=k_2t \quad \text{(Jander Model)} \quad (7)$$

$$1-(2/3)\,f-(1-f)^{2/3}=k_2t \quad \text{(Ginstling and Brounshtein Model)} \quad (8)$$

where, k_1: apparent kinetic constant for reaction control at the interface, k_2: apparent kinetic constant for diffusion control, t: Roasting time in minutes, f: potash recovery percentage and it can be calculated using Eq. (1).

The above three kinetic models were validated and the experimental data were fitted to the equations. The kinetic results were obtained by varying the temperature, time, keeping ratio of feldspar to additive ($CaCl_2$/NaCl) in 1 : 1 ratio and particle size at 45 μm constant. In the presence of both the additives the potash recovery value slowly increases with the increase of roasting time. The minimum was achieved at 700 °C and maximum was obtained at 950 °C over a maximum time period of 60 min. But a remark-

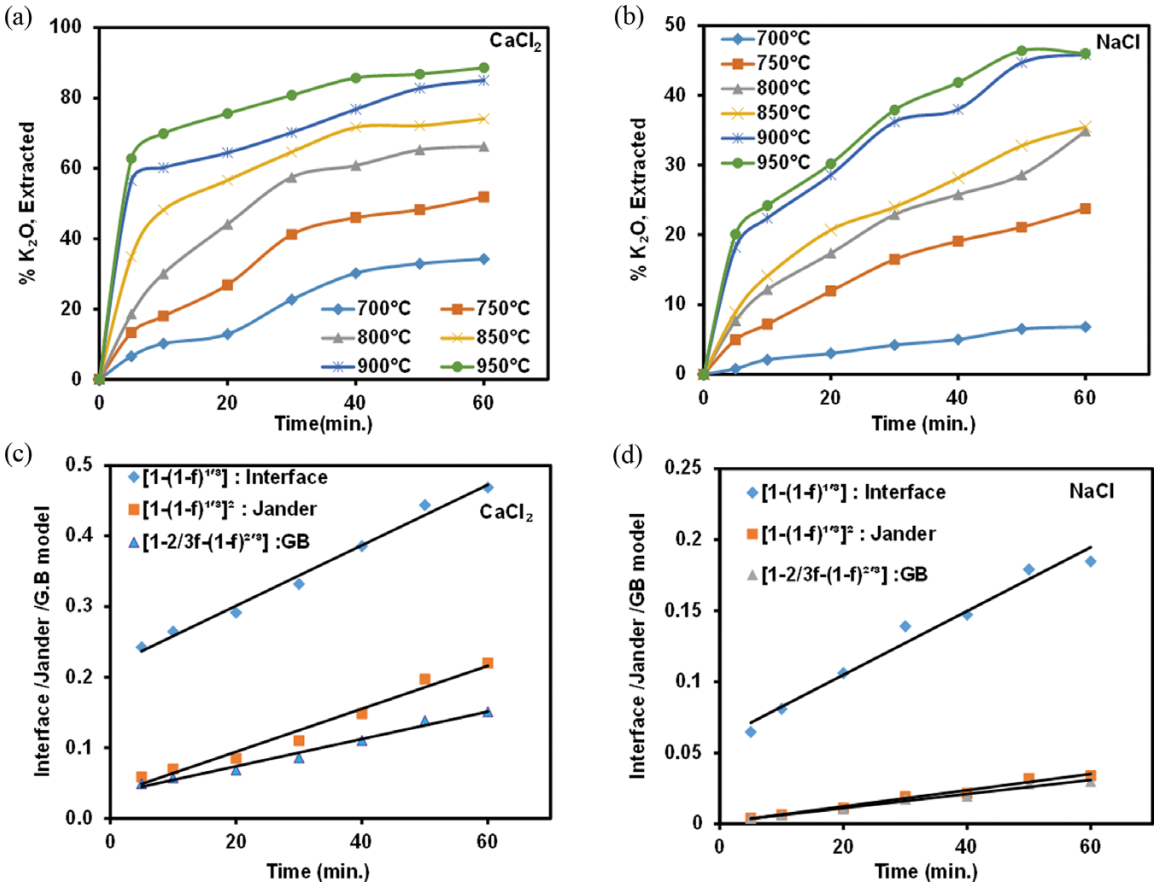


Fig. 13. Potash recovery at different temperatures and time intervals in presence of additives ((a) and (b)); plots of different kinetic models as a function of time at 900 °C ((c) and (d)).

able difference in recovery value was observed with respect to temperature. In the presence of $CaCl_2$, at all temperatures, the maximum potash recovery occurs within 30 min of roasting and beyond 30 min, a very slow increase in potash recovery is observed. But in the presence of NaCl roasting, very slow changes in recovery value take place with respect to time and temperature. This observation may be ascribed to the high melting point value of NaCl. The potash recovery at different temperatures and time intervals by NaCl and $CaCl_2$ and the different kinetic models is shown in Fig. 13.

The experimental results for NaCl and $CaCl_2$ were fitted to all the three models (Interface, Jander, and G.B) as a function of time at 900 °C (Fig. 13). The G.B model was found to validate the experimental data in comparison to the other models to a greater extent over the entire range of temperature (supported by the highest R^2 value). This GB model equation is further plotted at different temperatures as shown in Fig. 14. The relevant data of the three models at different temperatures are provided in Supplementary Table S4. The activation energies are calculated to be 90.27 kJ/mole and 122.24 kJ/mole for $CaCl_2$ and NaCl roasting processes, respectively, using the Arrhenius plot (Fig. 14(c)).

CONCLUSIONS

A comparative study of potash recovery from potash feldspar using two additives $CaCl_2$ and NaCl following the roast-leach method is described. Approximately 86% of potash recovery could be achieved by using $CaCl_2$ as the additive, whereas the use of NaCl as the additive provided 44% potash recovery under the same experimental conditions. Product analyses were carried out using XRD, SEM, FTIR, and Raman spectroscopic techniques to explain the results. The optimum recovery of potassium was accomplished when the roasting temperature, particle size, roasting time, and water leaching time were 900 °C, 45 μm, 60 min, and 15 min, respectively. The formation of new mineral phases such as sylvite, halite, and anorthite in the roasted products was established from the experimental data. The disappearance of water-soluble phases in the roast-leach residue was confirmed by the XRD studies. FT-IR and Raman studies confirmed the cleavage of tetrahedral rings of feldspar crystal during roasting with additives. Water leaching parameters such as leaching temperature, time of leaching, and temperature of leaching were insignificant because of the instantaneous water-soluble nature of sylvite formed during roasting. The experimental results were fitted to three kinetic models: Ginstiling-Brounstein kinetic model was found to be the best model. The activation energies for the roasting process were calculated to be 90 kJ/mole and 122 kJ/mole in the presence of $CaCl_2$ and NaCl, respectively. The overall data indicate the major roles of physical and chemical properties of additives in potash recovery from K-feldspar.

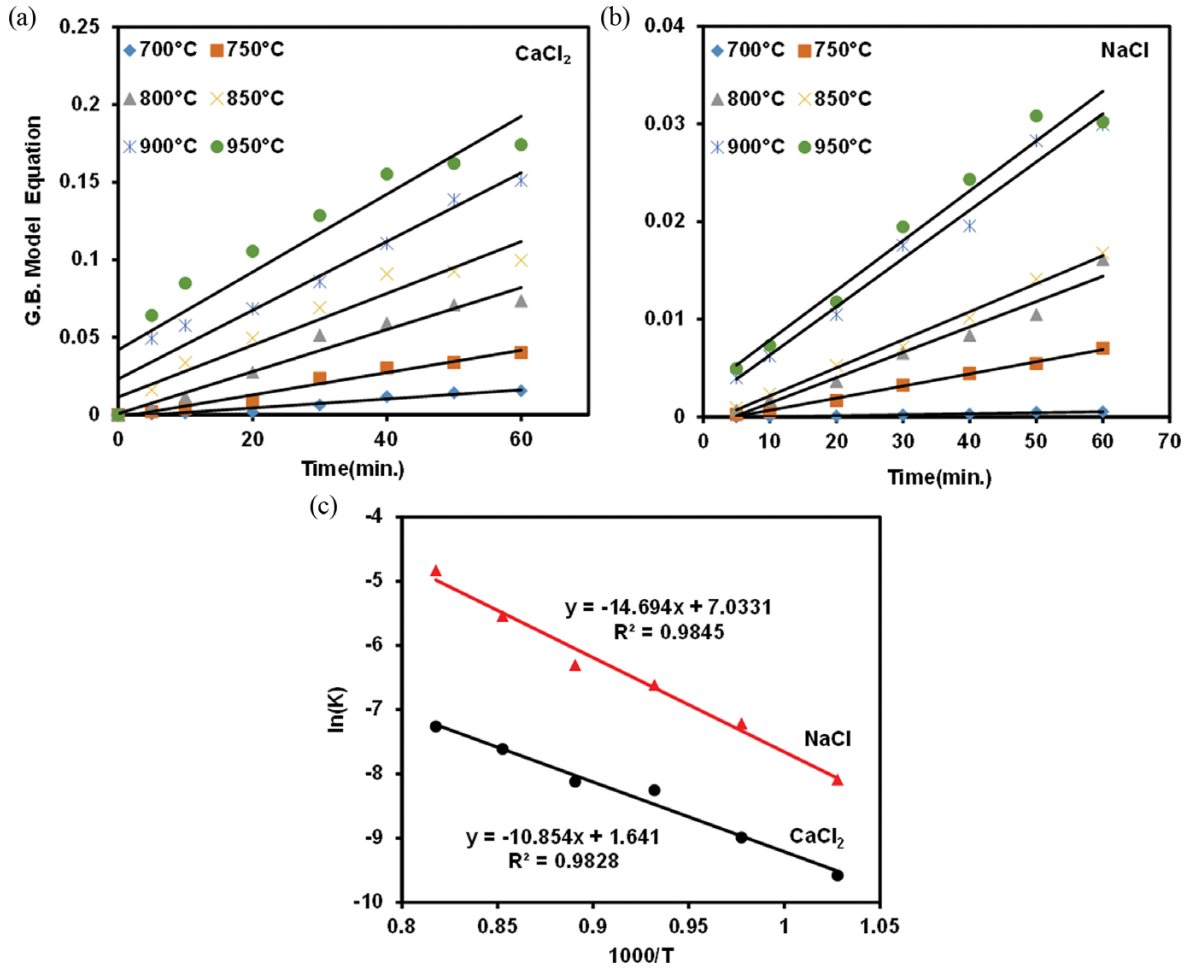


Fig. 14. Verification of the G.B. model equation ((a), (b)) and the Arrhenius plot (c) for roasting processes in presence of NaCl and $CaCl_2$.

ACKNOWLEDGEMENTS

The authors thank UGC (No.F.540/14/DRS/2013 (SAP-I)) and DST (SR/FST/CSII-021/2012(G)) for financial support to the School of Chemistry, Sambalpur University, India. The authors gratefully acknowledge the Director, CSIR-IMMT, Bhubaneswar, India for providing experimental facilities. Special thanks to Dr. Bisweswar Das, Chief Scientist, IMMT Bhubaneswar for useful discussions.

SUPPORTING INFORMATION

Additional information as noted in the text. This information is available via the Internet at http://www.springer.com/chemistry/journal/11814.

REFERENCES

1. S. R. Mousavi, M. T. Tavakoli, A. I. Chenari and M. Rezaie, *Adv. Environ. Biol.*, **8**, 10 (2014).
2. D. A. C. Manning, *Agr. Sustainable Dev.*, **30**, 2 (2010).
3. P. Heffer and M. Prudhomme, Fertilizer outlook 2016-2020, 84th IFA Annual Conference, Moscow-Russia (2016).
4. W. M. Stewart, D. W. Dibb, A. E. Johnston and T. J. Smyth, *Agron. J.*, **97**, 1 (2005).
5. R. C. Fluck, *Energy and alternatives for fertiliser and pesticides use*, chapter 13. Energy in farm production (2012).
6. J. Pretty and Z. P. Bharucha, *Ann. Bot.*, **114**, 8 (2014).
7. B. K. Kinekar, *Karnataka J. Agric. Sci.*, **24**, 1 (2011).
8. M. A. Hongwen, Y. Jing, S. Shuangging, L. Meitang, Z. Hong, W. Yingbin, Q. Hongb, Z. Pan and Y. Wengui, *Acta Geol. Sin.*, **89**, 6 (2015).
9. D. Ciceri, D. A. C. Manning and A. Allanore, *Sci. Total Environ.*, **502**, 590 (2015).
10. Y. Zhang, E. Asselin and Z. Li, *J. Chem. Eng. Jpn.*, **49**, 111 (2016).
11. J. A. Marinsky and Y. Marcus, *Ion exchange and solvent extraction*, Vol. 12, Marcel Dekker Inc., New York (1995).
12. A. Bajpayee, T. Luo, A. Muto and G. Chen, *Energy Environ. Sci.*, **4**, 1672 (2011).
13. J. Hou, J. Yuan and R. Shang, *Powder Technol.*, **226**, 222 (2012).
14. L. Pan, A. B. Zhang, J. Sun, Y. Ye, X. G. Chen and M. S. Xia, *Miner. Eng.*, **49**, 121(2013).
15. C. Karaguzel, I. Gulgonul, C. Demir, M. Cinarand and M. S. Celik, *Int. J. Miner. Process.*, **81**, 122 (2006).
16. G. W. Heyes, G. C. Allan, W. J. Bruckard and G. J. Sparrow, *Trans. Inst. Min. Metall.*, **C121**, 72 (2012).
17. O. Bayat, V. Arslan and Y. Cebeci, *Miner. Eng.*, **19**, 98 (2006).

18. Z. Sekulic, N. Canic, Z. Bartulovic and A. Dakovic, *Miner. Eng.*, **17**, 77 (2004).
19. G. R. Holdren and P. M. Speyer, *Am. J. Sci.*, **285**, 994 (1985).
20. S. Su, H. Ma and X. Chuan, *Adv. Powder Technol.*, **27**, 139 (2016).
21. S. K. Jena, N. Dhawan, D. S. Rao, P. K. Misra, B. K. Mishra and B. Das, *Int. J. Miner. Process.*, **133**, 13 (2014).
22. S. K. Jena, N. Dhawan, D. S. Rao, P. K. Misra and B. Das, *Sep. Sci. Technol.*, **51**, 269 (2016).
23. I. Styriakova, I. Styriak, P. Malachovsky and M. Lova, *Miner. Eng.*, **19**, 348 (2006).
24. A. Roy, S. K. Singh, P. C. Banerjee, K. Dana and S. K. Das, *Bull. Mater. Sci.*, **33**, 333 (2010).
25. I. Dogu and A. I. Arol, *Powder Technol.*, **139**, 258 (2004).
26. S. K. Jena, P. K. Misra and B. Das, *Miner. Process. Extr. Metall. Rev.*, **37**, 323 (2016).
27. A. K. Mazumder, T. Sharma and T. C. Rao, *Int. J. Miner. Process.*, **38**, 111 (1993).
28. S. Shekhar, D. Mishra, A. Agarwal and K. K. Sahu, *Appl. Clay Sci.*, **143**, 50 (2017).
29. J. R. Rao, R. Nayak and A. Suryanarayan, *Asian J. Chem.*, **10**, 690 (1998).
30. Z. Hao, S. Desi and B. Hong, *Adv. Mat. Res.*, **524-527**, 1136 (2012).
31. B. Yuan, C. Li, B. Liang, L. Lu, H. Yue, H. Sheng, L. Ye and H. Xie, *Chin. J. Chem. Eng.*, **23**, 1557 (2015).
32. X. Heping, W. Yufei, J. Yang, L. Bin, Z. Jiahua, Z. Ru, X. Lingzhi, L. Tao, Z. Xiangge, Z. Hongmei, L. Chun and L. Houfang, *Chinese Sci. Bull.*, **58**, 128 (2003).
33. S. K. Jena, N. Dhawan, S. S. Rath, D. S. Rao and B. Das, *Sep. Purif. Technol.*, **161**, 104 (2016).
34. R. Nayak, J. R. Rao, A. Suryanarayana and B. B. Nayak, *J. Sci. Ind. Res.*, **56**, 173 (1997).
35. P. L. G. Ladeira, World Intellectual Property Organisation, International Publication No - WO2013/061092 A1 (2013).
36. S. K. Liu, C. Han, J. M. Liu and H. Li, *RSC Adv.*, **113**, 5 (2015).
37. M. Kumanan, G. Sathya, V. Nandakumarand and L. J. Berchmans, *Extraction of potash from K-feldspar mineral by acid and molten salt leaching process*, July - Special Edition, www.iaset.us (2016).
38. W. U. Malik, G. D. Tuli and R. D. Madan, *Selected Topics in Inorganic Chemistry*, S. Chand and Sons Publisher, New Delhi - India (2010).
39. Anorthite, https://www.mindat.org.
40. H. Beherens and G. Muller, *Miner. Mag.*, **59**, 15 (1995).
41. Z. Lingdi, G. Jiugo, Y. Nianhua and L. Liyun, *Sci. China Ser. D.*, **40**, 159 (1997).
42. M. Zhang, E. K. H. Salje, M. A. Carpenter, I. Parsons, H. Kroll, S. J. B. Reed and A. Graeme-Barber, *Am. Miner.*, **82**, 9 (1997).
43. V. Bendel and B. C. Schmidt, *Eur. J. Miner.*, **20**, 1055 (2008).
44. J. J. Freeman, A. Wang, E. K. Kuebler, B. L. Jolliff and L. A. Haskin, *Can. Miner.*, **46**, 1477 (2008).
45. T. P. Mernagh, *J. Raman Spectros.*, **22**, 458 (1991).
46. A. Khawam and D. R. Flanagan, *J. Phys. Chem. B*, **110**, 17315 (2006).
47. E. Vitz, J. W. Moore, J. Shorb, X. P. Resina, T. Wendorff and A. Hahn, https://chem.libretexts.org/Ancillary_Materials/Exemplars_and_Case_Studies/Exemplars/Geology/Silicon_Dioxide_in_Earth's_Crust (2019).
48. T. Skorina and A. Allanore, *Green Chem.*, **17**, 2123 (2015).

Supporting Information

Competency of chlorination roasting coupled water leaching process for potash recovery from K-feldspar: Mechanism and kinetics aspects

Sandeep Kumar Jena[*,,†], Nilima Das[*], Akshaya Kumar Samal[***], and Pramila Kumari Misra[**,†]**

*CSIR-Institute of Minerals and Materials Technology, Bhubaneswar-751013, India
**School of Chemistry, Sambalpur University, Jyoti Vihar-768019, India
***Centre for Nano and Materials Sciences, Jain University, Bangalore-562 112, India
(*Received 4 June 2019 • accepted 22 September 2019*)

Table S1. Comparison table of alkali cations and their halides

Cation	Electronic configuration	Valency	Non-hydrated radius (A°)
K^+	$1S^2 2S^2 2P^6 3S^2 3P^6$	+1	1.33
Na^+	$1S^2 2S^2 2P^6$	+1	0.95
Ca^{+2}	$1S^2 2S^2 2P^6 3S^2 3P^6$	+2	0.99
Electronegativity difference and lattice energy of different halides			
Halide (XCl)	Electronegativity difference between X and Cl		Lattice energy of formation of XCl, kJ/mole
KCl	2.34		−715
NaCl	2.23		−786
$AlCl_3$	1.55		−2170
$SiCl_4$	1.26		−5492

Table S2. Water leaching experimental conditions

Experiment no	Parameters varied	Parameters fixed
1	% solid	Temperature, time, RPM
2	Temperature	% Solid, time, RPM
3	Time	Temperature, % solid, RPM
4	RPM	Temperature, time, % solid

Table S3. FTIR band position data [40-42]

Band position (cm^{-1})	Feldspar (bulk)
537.3	O-Si-O bending and K-O, Na-O stretching vibrations in microcline
587.2	O-Si(Al)-O bending vibrations
647.9	O-Si(Al)-O bending vibrations in microcline
729.5	Si-Si(Al) stretching vibrations
772.8	Si-Si stretching vibrations
1010.4	Si(Al)-O stretching vibration in microcline
1136.7	Si-O stretching vibration in microcline
Band position (cm^{-1})	Feldspar-$CaCl_2$ roast-leached residue
537.2	This peak appears almost in the same position as in bulk, but the intensity is lowered or weak after roasting followed by leaching
601.5	The peak at 587.2 as in bulk has moved to a higher wavelength region of 601.5, indicating the disorderness of bending vibrations in O-Si(Al)-O
647.9	Completely disappeared, indicating the breaking of O-Si (Al)-O bond in the crystal structure
722.6/775.9	Comparatively broad and weak than the bulk peak
946.9/1098.2	Moves to a low wave number position than the bulk
1098.2	Si-O stretching Vibration in albite
Band position (cm^{-1})	Feldspar-NaCl roast-leached residue
533.8	This peak becomes more sharper than the bulk peak
598.0	Moves to a higher wavelength region
733.0/769	The two sharp and well-defined peaks become broader and seem to be completely disappeared
1035.6	Moves to higher wavelength region compared to bulk, this band appears due to Si(Al)-O stretching vibration in albite
1158	This peak appears due to Si-O stretching Vibration in albite, which was also further confirmed by XRD spectra

Table S4. R^2 values for $NaCl/CaCl_2$ roasting process

Models	Interface controlled reaction		Jander model		G.B. model	
Temp. (in ^oC)	NaCl	$CaCl_2$	NaCl	$CaCl_2$	NaCl	$CaCl_2$
700	0.9785	0.9595	0.9689	0.9584	0.9796	0.9789
750	0.9790	0.9490	0.9940	0.9752	0.9950	0.9923
800	0.9840	0.9161	0.9600	0.9642	0.9850	0.9897
850	0.9816	0.9122	0.9922	0.9533	0.9941	0.9827
900	0.9740	0.9889	0.9818	0.9741	0.9885	0.9929
950	0.9548	0.9592	0.9691	0.9791	0.9782	0.9867